Journal of Materials Chemistry A

Accepted Manuscript

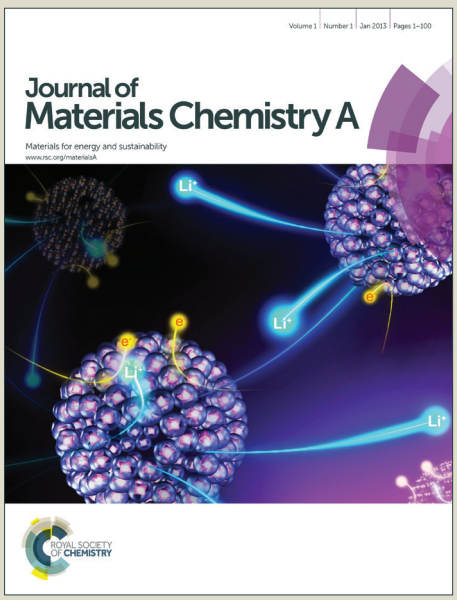

This is an *Accepted Manuscript*, which has been through the Royal Society of Chemistry peer review process and has been accepted for publication.

Accepted Manuscripts are published online shortly after acceptance, before technical editing, formatting and proof reading. Using this free service, authors can make their results available to the community, in citable form, before we publish the edited article. We will replace this *Accepted Manuscript* with the edited and formatted *Advance Article* as soon as it is available.

You can find more information about *Accepted Manuscripts* in the Information for Authors.

Please note that technical editing may introduce minor changes to the text and/or graphics, which may alter content. The journal's standard Terms & Conditions and the Ethical guidelines still apply. In no event shall the Royal Society of Chemistry be held responsible for any errors or omissions in this *Accepted Manuscript* or any consequences arising from the use of any information it contains.

ROYAL SOCIETY OF CHEMISTRY

www.rsc.org/materialsA

Journal Name

RSCPublishing

ARTICLE

Selective, sensitive, and reversible H_2S sensors using Mo-doped ZnO nanowire networks†

Cite this: DOI: 10.1039/xoxxoooooox

Hyung-Sik Woo,[a] Chang-Hoon Kwak,[a] Il-Doo Kim[b] and Jong-Heun Lee*[a]

Received ooth January 2012,
Accepted ooth January 2012

DOI: 10.1039/xoxxoooooox

www.rsc.org/

The Mo-doped ZnO nanowire (NW) networks were prepared by coating the MoS_2 layer through successive ionic layer adsorption and reaction and subsequent heat treatment at 600°C for 2 h. The resulting Mo-doped ZnO NW network sensor demonstrated a high gas response of 14.11 to 5 ppm H_2S at 300°C, which is 7.66–11.47 times higher than those of 5 ppm C_2H_5OH, NH_3, HCHO, CO, H_2, *o*-xylene, benzene, toluene, and trimethylamine. The reversibility of the sensor signal, as well as the response and selectivity to H_2S, is significantly improved by Mo doping into the ZnO NW networks, which can open various applications to monitor H_2S in indoor atmosphere, industrial petroleum/gas, and automobile exhaust gas.

1. Introduction

Hydrogen sulfide (H_2S) is a colorless, flammable, and extremely poisonous gas with a rotten-egg-like smell; it is formed naturally in crude petroleum, natural gas, automobile exhaust gas, and hot springs.[1–3] According to the US Occupational Safety and Health Administration,[4] human exposure to low concentrations of H_2S can cause irritation to the eyes, nose, throat, and respiratory system, while increased concentrations can cause more severe eye and respiratory irritation, headache, nausea, shock, rapid unconsciousness, coma, and even death. There is, therefore, a growing need for gas sensing devices that can detect H_2S gas at low concentrations.

Three key requirements of gas sensors are gas response, selectivity, and reliability. Single crystalline ZnO nanowires (NWs) have been intensively investigated as a promising material platform for sensitive and stable gas sensors due to their high surface area to volume ratio and excellent thermal stability at high operation temperature.[5,6] Gas sensing characteristics of ZnO NWs can be further tuned or enhanced by surface modification via coating the discrete[7] or continuous overlayer.[8] Various n-type oxide semiconductors such as SnO_2, ZnO, In_2O_3, and WO_3 have been explored as potential sensing materials to detect ppm-level H_2S.[9-12] In general, the pure sensing materials do not provide selective detection of H_2S. The loading of n-type oxide semiconductors with CuO has previously been suggested as an efficient approach to enhance both the response and selectivity to H_2S.[13-15] However, the recovery of such sensors was quite often found to be sluggish, or even incomplete, which is ascribed to the sluggish oxidation of CuS (formed by the reaction between CuO and H_2S) and/or the deterioration of the sensing surface by sulfur compounds.[16,17] This says that high performance H_2S sensors exhibiting high response, excellent selectivity, and good reversibility simultaneously remains challenging and should be designed using a new additive. MoO_3 is known to form non-reactive, thus, regenerable adsorption of H_2S.[18] Moreover, the potential of Mo as the additive to control the selectivity to H_2S was demonstrated by the sensor using MoO_3-ZnO nano-composites.[19]

In this paper, Mo is proposed as an effective dopant for the design of selective and sensitive H_2S sensors, without sacrificing their reversible sensing behavior. To this end, ZnO nanowire networks were doped with Mo by successive ionic layer adsorption and reaction (SILAR), and their H_2S sensing characteristics were investigated. High performance sensing characteristics of Mo-doped ZnO NW can pave a new way to monitor H_2S in indoor air atmosphere, industrial petroleum/gas, and automobile exhaust gas. The focus of this work is directed at understanding the reasons for the superior H_2S sensing characteristics of Mo-doped ZnO NW networks.

2. Experimental

2.1 Sample preparation

ZnO NWs were directly grown on alumina substrates with two gold electrodes by carbothermal reduction, using a mixture of ZnO (99.9 %, Sigma Aldrich) and graphite (< 20 μm, Sigma Aldrich) powders. An alumina boat containing the source powders was first placed in the middle of the quartz tube of a horizontal tube furnace, and the alumina substrates with the gold electrodes were placed 5 cm downstream of the source material. The two gold electrodes acted as catalyst for the growth of ZnO NWs by the vapor-liquid-solid mechanism, which resulted in a highly porous NW network with good electrical contact with the electrodes (Fig. 1a). The ZnO NWs

[a]*Department of Materials Science and Engineering, Korea University,Seoul, 136-713, Republic of Korea. E-mail: jongheun@korea.ac.kr*

[b]*Department of Materials Science and Engineering, Korea Advanced Institute of Science and Technology, Daejeon 305-701, Republic of Korea*

†*Electronic Supplementary Information (ESI) available:*

Journal of Materials Chemistry A Accepted Manuscript

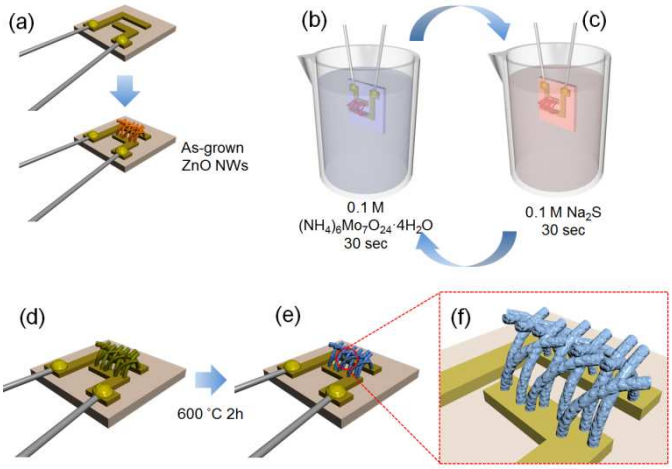

Fig. 1 Fabrication of Mo-doped ZnO NW networks by the SILAR method.

were grown at 900°C for 20 min in Ar/O_2 mixture gas, while the pressure of the quartz tube was maintained at ~1 × 10^{-2} torr by mechanical pumping.

The MoS_2 layer was uniformly coated on the surfaces of the ZnO NWs by SILAR method which was modified from that suggested by Sartale and Lokhande.[20] A 0.1 M ammonium molybdate [$(NH_4)_6Mo_7O_{24}\cdot 4H_2O$] solution (temperature: 16°C) and 0.1 M sodium sulfide (Na_2S) solution (temperature: 16°C) were used as the source materials for deposition, and the pH of the ammonium molybdate was adjusted to 3.0 by the addition of diluted H_2SO_4. The alumina substrate with as-grown ZnO NWs was first dipped into the ammonium molybdate solution for 30 s (Fig. 1b), rinsed with deionized water, and then dipped into the sodium sulfide solution for 30 s (Fig. 1c). This procedure was repeated 10 times; the MoS_2-coated ZnO NWs (Fig. 1d) were then heat treated at 600°C for 2 h in air to form the final Mo-doped ZnO NWs (Fig. 1e and f).

2.2 Characterization

The phases and crystallinity of the synthesized NWs were analyzed by X-ray diffraction (XRD, Rigaku D/MAX-2500V/PC); the morphologies of pristine and Mo-doped ZnO NWs, by field-emission scanning electron microscopy (FE-SEM, S-4800, Hitachi Co. Ltd., Japan) and transmission electron microscopy (TEM, FEI Titan); and the chemical state of pure ZnO NWs and Mo-doped ZnO NWs, by X-ray photoelectron spectroscopy (XPS, X-TOOL, ULVAC-PHI).

2.3 Gas sensing characteristics

Sensor elements with NW networks were heat treated at 600°C for 2 h to decompose any organic material on the sensor substrate. The sensor was then placed in a quartz tube and the temperature of the furnace was stabilized at 300°C, and a flow-through technique with a constant flow rate of 500 cm^3min^{-1} was used. The gas responses ($S = R_a/R_g$, R_a: resistance in air, R_g: resistance in gas) to 5 ppm H_2S, C_2H_5OH, NH_3, HCHO, CO, H_2, *o*-xylene, benzene, toluene, and trimethylamine (TMA) were all subsequently measured at 300–400°C. The dc resistance of the sensor was measured in dry atmosphere using an electrometer, interfaced with a computer.

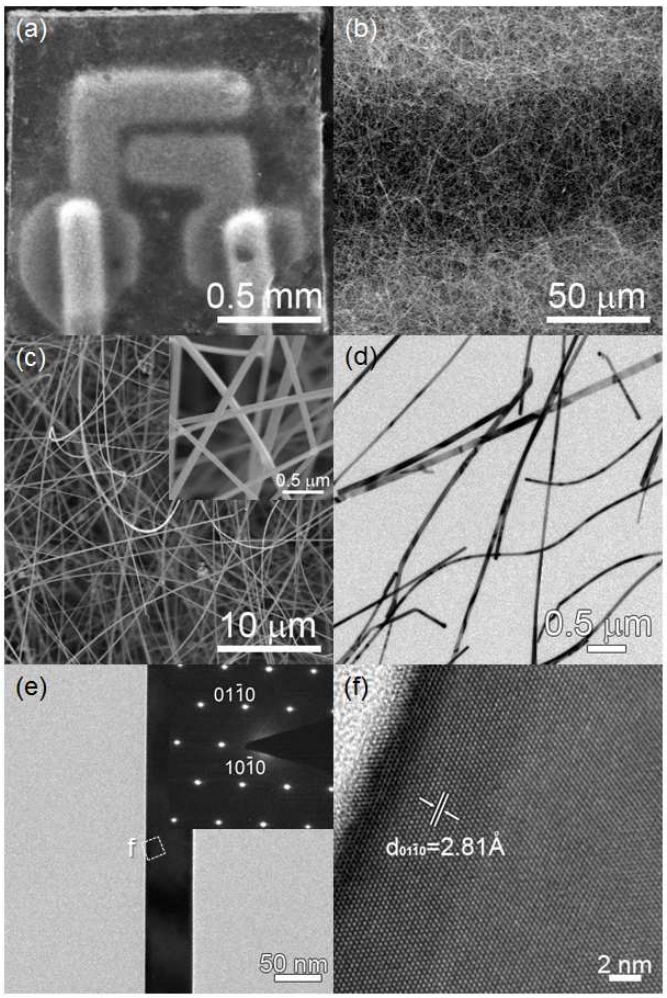

Fig. 2 (a-c) SEM and (d-f) TEM images of pristine ZnO NW network sensors.

3. Result and discussion

3.1 Growth and characterization of pure and Mo-doped ZnO nanowire network

The single crystalline ZnO NWs grown on alumina substrate are shown in Fig. 2a and 2b. The diameter of the NWs ranged from 50 to 80 nm, while the length was in the order of several tens of micrometers (Fig. 2c and d). It is also worth noting that the pristine ZnO NWs exhibit clean surfaces. The selective area electron diffraction (SAED) pattern confirms that the single crystalline ZnO NWs were grown in the [01$\bar{1}$0] direction (Fig. 2e) and the high-resolution image of a single NW showed highly crystalline (01$\bar{1}$0) fringes separated by 2.81 Å (Fig. 2f).

After treatment with ammonium molybdate and sodium sulfide solutions, the surface of the substrate was found to be covered with a gel-like MoS_2 (Fig. 3a), which was subsequently converted into NWs with a rough surface morphology (Fig. 3b-d) by heat treatment at 600°C. Heat treatment did not change the overall NW network structures. Small protrusions on the surface of NWs (Fig. 3e and f) exhibit ZnO (01$\bar{1}$0) fringes separated by 2.81 Å, with a crystalline Fast Fourier Transformation pattern (Fig. 3f). All the protrusions observed during TEM analysis were identified not as MoO_3, but as ZnO (Fig. S1). The MoS_2 coating on the ZnO NWs can be transformed into MoO_3 by heat treatment, and thus MoO_3-decorated

Journal of Materials Chemistry A Accepted Manuscript

This journal is © The Royal Society of Chemistry 2012

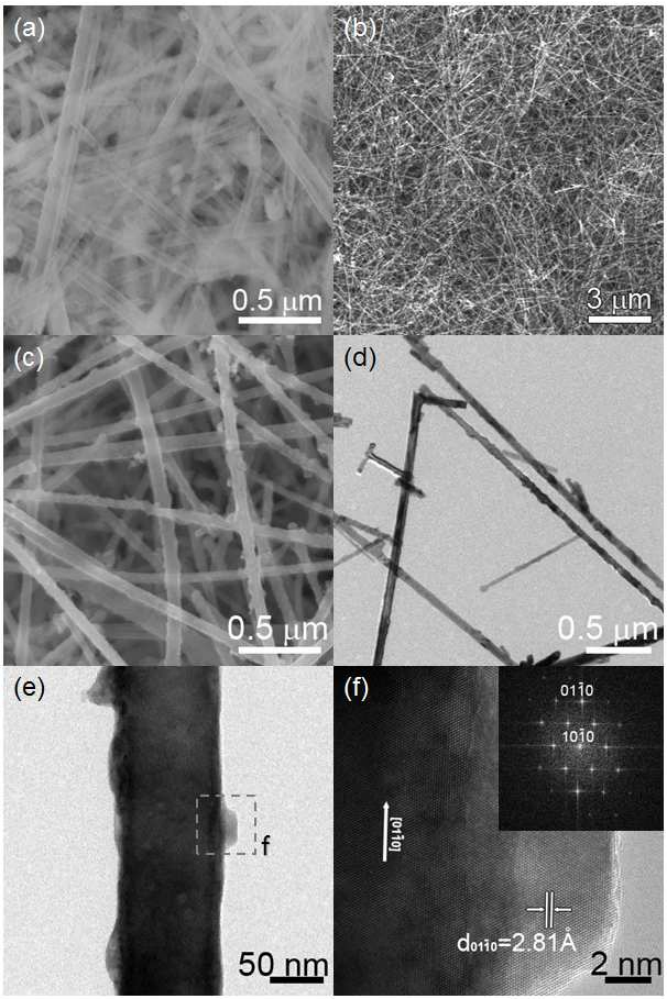

Fig. 3 (a) SEM image of MoS_2-coated ZnO NW networks, (b,c) SEM and (d,e) TEM images of Mo-doped ZnO NW networks after heat treatment at 600°C, and (f) lattice image of dotted area in (e) and fast Fourier transform.

ZnO NWs can potentially be formed when no reaction occurs between MoO_3 and ZnO. However, the absence of a MoO_3 phase near the protrusions indicates that a strong chemical reaction, i.e., the incorporation of Mo into ZnO lattices, is likely to have occurred prior to the formation of MoO_3. The ionic radius of Zn^{2+}, with the coordination number of 4, in the literature ranges from 0.074 to 0.083 nm, while that of Mo^{6+} with the same coordination number in the literature ranges from 0.055 to 0.062 nm.[21,22] The highest solubility limit of Mo^{6+} in ZnO lattice has been reported to be 4 at%;[23] however, the incorporation mechanism remains unclear due to both substitution and interstitial Mo^{6+} having been suggested.[21,22,24] From TEM analysis and the literature, Mo-doped ZnO NWs are believed to be formed by high-temperature heat treatment. Indeed, the presence of Mo was confirmed in the NWs by energy dispersive X-ray spectroscopy (EDS) analysis. The average Mo concentration of 10 different NW regions was calculated to be $[Mo^{6+}]/([Zn^{2+}]+[Mo^{6+}]) = 2.2 \pm 0.6$ at% (Fig. S2) from the EDS analysis, which is substantially lower than the solubility limit.

The diffusivity of Zn^{2+} in ZnO at 600°C is 1.92 x 10^{-16} cm^2/s, though no comparable diffusivity of Mo^{6+} in ZnO is available in the literature. If the diffusivity of Mo^{6+} is significantly higher than that of Zn^{2+}, Mo-doped ZnO NWs would be formed with a relatively clean surface morphology. If, however, the outward diffusion of Zn^{2+} is dominant over the inward diffusion of Mo^{6+}, then the ZnO NWs would be expected to have rough surfaces, with a gradient of Mo concentration being created from the surface (Mo-enriched region) to the core of the NWs. Finally, if both the diffusion of Mo^{6+} and Zn^{2+} are similarly rapid, then Mo-doped ZnO NWs with a rough surface and uniform distribution of Mo dopant should be obtained. Local EDS analysis revealed a higher Mo concentration in the outer region of NWs (Fig. S3), indicating that the diffusion of Mo is insufficient to permit homogeneous doping of Mo throughout the ZnO NWs. It is, however, worth noting that a higher Mo concentration near the surface of the NW can be advantageous in terms of its catalytic effect upon exposure to H_2S gas.

Pure ZnO NWs were identified as a wurtzite phase (JCPDS 36-1451), with primary peaks of (101), (100), and (002) (Fig. S4a). The intensity of (002) peak became relatively higher after dipping of ZnO NW networks in the Mo and S precursor solutions (Fig. S4b) although neither Mo nor S containing phases was observed in the substrates. This can be explained by the preferred coating of the low crystalline MoS_2 phase on the (101) and (100) surfaces of ZnO NWs and/or the presence of MoS_2 being below the detection limit of X-ray diffraction although further study is needed to confirm this. No MoO_3 phase was found by X-ray diffraction after heat treatment (Fig. S4c), indicating that Mo was incorporated into the ZnO lattice.

The existence of MoS_2 and Mo, and their oxidation states, was investigated by XPS, both before and after heat treatment (Fig. 4). Prior to heat treatment, the ZnO NWs after SILAR exhibited S2*s* (225.7 eV) (Fig. 4a) and S2*p* peaks at 162.4 and 161.3 eV (Fig. 4b), which correspond to $S2p_{1/2}$ and $S2p_{3/2}$ doublets, respectively.[25,26] Two Mo3*d* peaks were observed at 229.7 and 232.9 eV, which can be attributed to the doublet of $Mo^{4+}3d_{5/2}$ and $Mo^{4+}3d_{3/2}$ (Fig. 4a), while the presence of S2s and S2p peaks confirms the formation of

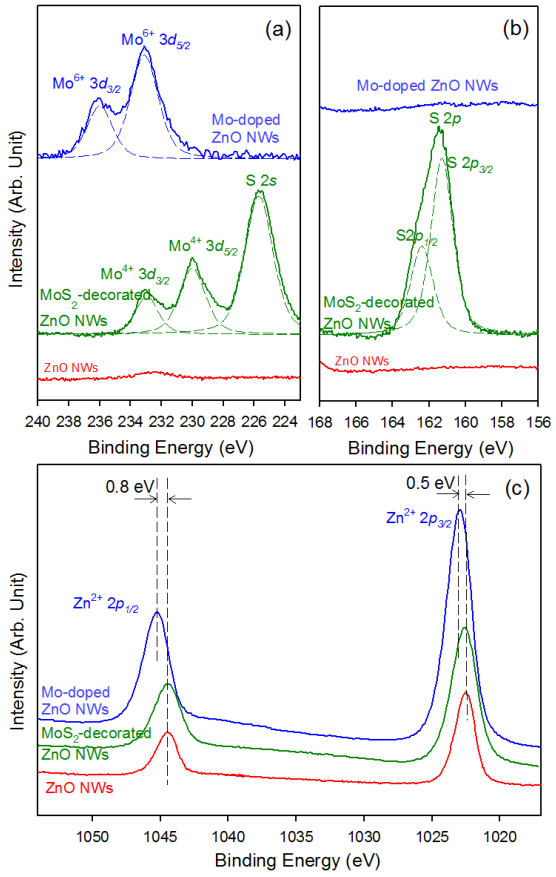

Fig. 4 XPS spectra of pristine, MoS_2-coated and Mo-doped ZnO NWs.

Journal of Materials Chemistry A Accepted Manuscript

MoS_2 after the SILAR process.[27] Following heat treatment, Mo3*d* peaks of $Mo^{6+}3d_{5/2}$ and $Mo^{6+}3d_{3/2}$ doublets were observed at 233 and 236 eV, respectively, which are indicative of the presence of Mo^{6+}.[28] The $Zn2p_{3/2}$ and $Zn2p_{1/2}$ peaks are also shifted to a higher binding energy with a value of 0.5–0.8 eV (Fig. 4c) as a result of heat treatment, which can be explained by the difference in electronegativity (χ) of Zn (χ=1.65) and Mo (χ=2.16). This comparably higher electronegativity of Mo attracts electrons from Zn, resulting in a decrease in its electron screening effect.[29] This confirms that Mo^{6+} is doped to the ZnO lattice, without the formation of a MoO_3 phase.

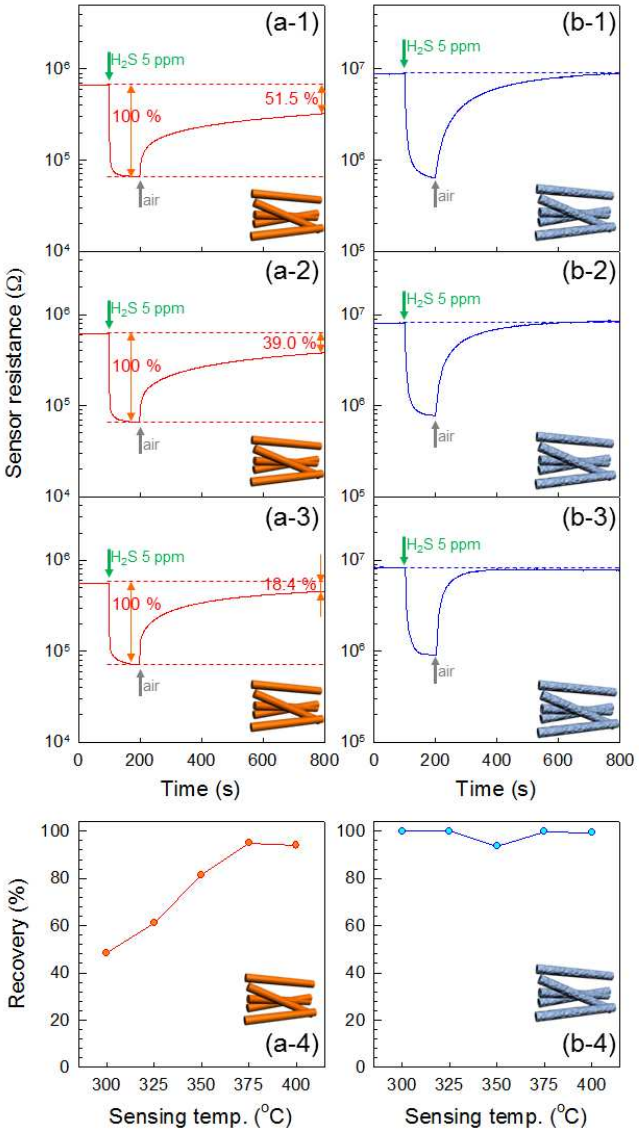

Fig. 5 Sensing transients of pure and Mo-doped ZnO NW network gas sensors to 5 ppm H_2S at 300, 325, and 350°C: (a-1) ZnO NW sensor, 300°C, (a-2) ZnO NW sensor, 325°C, (a-3) ZnO NW sensor, 350°C, (b-1) Mo-doped ZnO NW sensor, 300°C, (b-2) Mo-doped ZnO NW sensor, 325°C, (b-3) Mo-doped ZnO NW sensor, 350°C. (a-4) and (b-4) *Recovery (%)* = ($R_{air\text{-}recovery}$ − $R_{gas\text{-}H2S}$) /($R_{air\text{-}fresh}$ − $R_{gas\text{-}H2S}$) x 100 (%) of pure and Mo-doped ZnO NW sensor at 300–400°C (where, $R_{air\text{-}fresh}$: sensor resistance in air before exposure to H_2S, $R_{gas\text{-}H2S}$: sensor resistance in 5 ppm H_2S, and $R_{air\text{-}recovery}$: sensor resistance in air after 10 min exposure to air).

3.2 Gas sensing characteristics

The gas sensing characteristics were measured in order to investigate the catalytic effect of Mo doping on the gas sensing characteristics of ZnO NWs (Fig. 5). Both pure and Mo-doped ZnO NW sensors exhibited typical n-type gas sensing characteristics, that is, a decrease and increase in sensor resistance upon exposure to a reducing gas and air, respectively. After sensing reactions with sulfur-free analyte gases such as 5 ppm C_2H_5OH, NH_3, HCHO, CO, H_2, *o*-xylene, benzene, toluene, and trimethylamine, the resistance of the pure ZnO NW network sensor was completely returned to that measured in air by simply removing the analyte gas (Fig. S5), which is consistent with the literature.[30-33] However, the sensor resistance did not return to the sensor resistance in air even after exposure to ambient air for 10 min next to H_2S sensing. Thus, the irreversible sensing characteristics in Fig. 5a might emanate from sulfur component in H_2S. This irreversibility tended to become stronger as the sensor temperature decreased from 400 to 300°C. For example, the sensing and recovering transients to 5 ppm H_2S at 300, 325, and 350°C are shown in Fig. 5a-1, 5a-2 and 5a-3. In sharp contrast, the resistance of the Mo-doped ZnO NW sensor completely recovered within only a short period of time at sensing temperatures of 300–350°C (Fig. 5b-1, 5b-2 and 5b-3). As a measure of the irreversibility in the sensor signal during recovery, *Recovery (%)* = ($R_{air\text{-}recovery}$ − $R_{gas\text{-}H2S}$)/($R_{air\text{-}fresh}$ − $R_{gas\text{-}H2S}$) x 100 (%) (where $R_{air\text{-}fresh}$: sensor resistance in air before exposure to H_2S, $R_{gas\text{-}H2S}$: sensor resistance in 5 ppm H_2S, and $R_{air\text{-}recovery}$: sensor resistance in air after 10 min exposure to air) has been calculated (Fig. 5a-4 and 5b-4). The *recovery (%)* values of a pure ZnO NW sensor at 300, 325, and 350°C were 48.49, 61.00, and 81.58, respectively (Fig. 5a-4), while those of a Mo-doped ZnO NW sensor were near to 100 % over the entire range of sensing temperatures tested (300-400°C) (Fig. 5b-4).

The responses of pure and Mo-doped ZnO NW sensors to various reducing gases were measured at 300–400°C (Fig. 6a and b). In the case of a pure ZnO NW sensor, the response to 5 ppm H_2S (R_a/R_g = 6.73–9.58) is higher than those to 5 ppm C_2H_5OH (R_a/R_g = 2.15–5.13), NH_3 (R_a/R_g = 2.21–3.32), HCHO (R_a/R_g = 1.97–4.1), CO (R_a/R_g = 1.58–2.75), H_2 (R_a/R_g = 2.11–2.92), *o*-xylene (R_a/R_g = 1.38–2.42), benzene (R_a/R_g = 1.8–2.42), toluene (R_a/R_g = 1.44–1.82), and trimethylamine (R_a/R_g = 1.59–3.53) (Fig. 6a). The selectivity for H_2S was found to be maximum at 325°C, which tended to decrease as the sensor temperature was raised to 400°C. However, the selective detection of H_2S at 300–350°C is unsuitable for practical application given the incomplete recovery at such temperatures (Fig. 5a-1, 5a-2 and 5a-3). On the other hand, at sensor temperatures of 375 and 400°C, the selective detection of H_2S is limited by the relatively high cross responses to C_2H_5OH and HCHO.

In the Mo-doped ZnO NW sensors, the response to H_2S showed a maximum value (R_a/R_g = 14.11) at 300°C, which decreased with increasing sensor temperature (Fig. 6b). In general, the cross-response to other reducing gases was reduced by the Mo doping (Fig. 6a and 6b), which accounts for the highest selectivity for H_2S being achieved at 300°C (Fig. 6c). The response to 5 ppm H_2S at 300°C was found to be 7.66–11.47 times higher than those to other reducing gases (R_a/R_g = 1.23–1.84). Furthermore, the response of the Mo-doped ZnO NW sensor to 0.2–5 ppm H_2S ranged from 2.67 to 14.11,

Journal of Materials Chemistry A Accepted Manuscript

This journal is © The Royal Society of Chemistry 2012

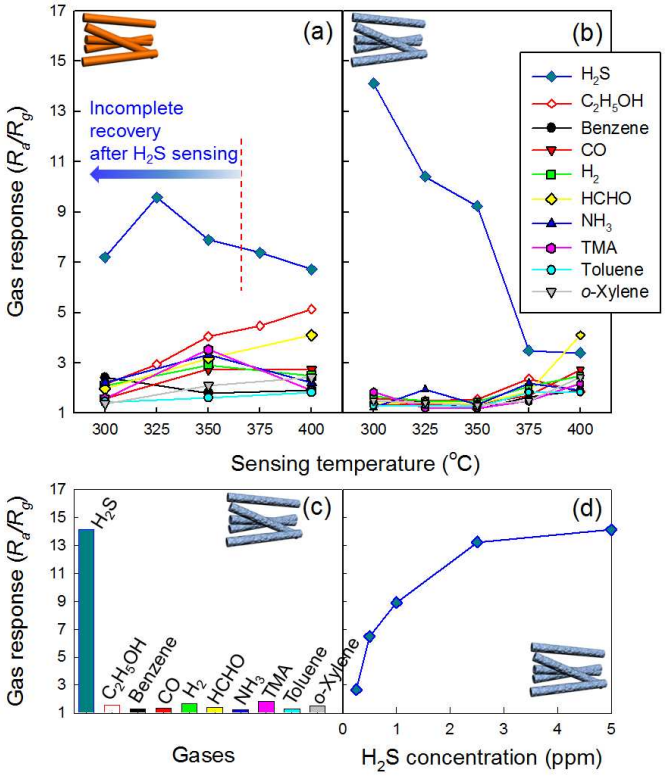

Fig. 6 Gas response of (a) a pure ZnO NW network sensor and (b) a Mo-doped ZnO NW network sensor to 5 ppm H_2S, C_2H_5OH, benzene, CO, H_2, HCHO, NH_3, trimethylamine, toluene, and *o*-xylene at 300–400°C; (c) gas selectivity of Mo-doped ZnO NW network sensor at 300°C and (d) gas responses to 0.2–5 ppm H_2S at 300°C.

indicating that the H_2S detection limit of the sensor is lower than 0.2 ppm (Fig. 6d). It is also worth noting that the Mo-doped ZnO NW sensor shows complete recovery after repetitive sensing of different concentration of H_2S, even at a relatively low sensing temperature (Fig. S6). Accordingly, a Mo-doped ZnO NW sensor could be used to detect trace concentrations of H_2S in a sensitive, selective, and reversible manner.

3.3 Discussion

The resistance of n-type oxide semiconductor is significantly increased by the formation of electron depletion layer near the surface due to the adsorption of oxygen with negative charge such as O_2^-, O^-, and O^{2-}.[34] Thus, the reaction between reducing gas and negatively charged surface oxygen leads to the decrease of sensor resistance.[5,34,35] The ionized species of adsorption are dependent upon the sensing temperature. In general, at the sensor temperature of present study (300-400°C), the O^- and O^{2-} are known as dominant species.[34,36,37] The decrease of sensor resistance upon exposure to H_2S in the present study can be attributed to the increase of electron concentration by the reaction between H_2S and O^-/O^{2-}.

Various metal oxide semiconductors such as SnO_2, Fe_2O_3, In_2O_3, Cu_2O, WO_3, TiO_2 have been previously explored as sensing materials for the detection of H_2S.[9-12,38-42] Numerous published papers have reported incomplete recovery when purging with air after H_2S sensing, and hence, additional procedures such as UV irradiation or heating have been suggested to increase the recovery of the sensor.[43,44] This lack of recovery has also been a key issue in several ZnO gas sensors, which is again confirmed by the present results of a pure ZnO NW sensor. Finding a solution to this issue of semiconductor gas sensor recovery after H_2S detection is, therefore, believed to be of paramount importance for the precise and continuous detection of H_2S.

Matsuda et al.[18] suggested two types of oxide adsorbents for H_2S adsorption, i.e., non-regenerable and regenerable. ZnO, CuO, and Fe_2O_3 are commonly known as non-regenerable adsorbents, which support the irreversible H_2S sensing behavior of pure ZnO NW sensors. The non-regenerable oxide adsorbents, such as ZnO and CuO, are converted into ZnS and CuS by a reactive adsorption that involves chemical reaction. However, the conversion from sulfide to oxide upon exposure to air generally takes a prolonged time, or leads to incomplete recovery. In contrast, MoO_3 is known to form non-reactive adsorption, such as $MoO_3{\cdot}SH_2$ and $MoO_2{\cdot}S$, by reaction with H_2S at 100–300°C and the oxide surface can be easily regenerated by the desorption of H_2S.[18] This relatively easy adsorption of H_2S on the surface of Mo oxides suggests a chemical affinity between the two, which may be the reason for the high selectivity and response to H_2S in the Mo-doped ZnO NW sensor. The high selectivity and response to H_2S observed in the Mo-doped ZnO NW sensor of the present study can therefore be attributed to the high chemical affinity of Mo oxide to H_2S, and the regenerable adsorption/desorption of the Mo oxide surface. The MoS_2, which is known as chemoresistive n-type oxide semiconductor,[45] might be formed on the surface of Mo-doped ZnO NWs by the reaction between Mo component and H_2S. However, considering that the concentration of both dopant Mo (~ 2.2 at%) and analyte gas (H_2S 5 ppm) are very low, the formation of continuous MoS_2 layer for conduction and its contribution to gas sensing characteristics is less plausible although further detailed study is necessary to substantiate this.

Many semiconductor gas sensors show a relatively high response towards C_2H_5OH gas,[46-50] and consequently, the selective detection of other gases becomes more difficult. It is known that C_2H_5OH is dehydrated into the more reactive $CH_3CHO_{(gas)} + H_{2\,(gas)}$ at the surface of a basic oxide, while it is dehydrogenated into the less reactive $C_2H_{4\,(gas)} + H_2O_{(gas)}$ at the surface of an acidic oxide.[51] In the present study, the significant decrease in cross-response to 5 ppm C_2H_5OH from 5.13 to 1.84, at a sensor temperature of 400°C, can be attributed to the Mo-induced suppression of the C_2H_5OH sensing reaction. The Mo doping, therefore, not only increases the response towards H_2S, but also decreases cross-responses towards other gases, thus resulting in the highly selective detection of H_2S gas.

4. Conclusion

The Mo-doped ZnO NWs were prepared by coating MoS_2 layer on ZnO NWs using the SILAR method, followed by heat treatment at 600°C. The sensor using Mo-doped ZnO NW networks exhibited not only a high gas response and selectivity towards H_2S gas, but also full recovery after detection. Meanwhile, a pristine ZnO sensor showed incomplete recovery after H_2S sensing at 300–350°C. The high selectivity and response to H_2S were explained by the strong chemical interaction between Mo oxide and H_2S, while the reversible H_2S sensing characteristics were explained by the regenerable adsorption/desorption of H_2S on the Mo oxide surface.

Journal of Materials Chemistry A Accepted Manuscript

Acknowledgments

This work was supported by the National Research Foundation of Korea (NRF), grant funded by the Korean government (MEST) (No. 2013R1A2A1A01006545).

Notes and references

1 S. F. Watts, *Atmospheric Environment*, 2000, **34**, 761–779.
2 D. Gabriel and M. A. Deshusses, *Proceedings of the National Academy of Sciences of the United States of America*, 2003, **100**, 6308–6312.
3 I.-S. Hwang, J.-K. Choi, S.-J. Kim, K.-Y. Dong, J.-H. Kwon, B.-K. Ju and J.-H. Lee, *Sens. Actuators, B*, 2009, **142**, 105–110.
4 *Occupational Safety and Health Administration*, http://www.osha.gov/
5 O. Lupan, V. V. Ursaki, G. Chai, L. Chow, G. A. Emelchenko, I. M. Tiginyanu, A. N. Gruzintsev and A. N. Redkin, *Sens. Actuators, B*, 2010, **144**, 56–66.
6 Q. Wan, Q. H. Li, Y. J. Chen, T. H. Wang, X. L. He, J. P. Li and C. L. Lin, *Appl. Phys. Lett.*, 2004, **84**, 3654–3656.
7 C.W. Na, H.-S. Woo, I.-D. Kim and J.-H. Lee, *Chem. Commun.*, 2011, **47**, 5148–5150.
8 N. Singh, A. Ponzoni, R. K. Gupta, P. S. Lee and E. Comini, *Sens. Actuators, B*, 2011, **160**, 1346–1351.
9 H. Liu, S. P. Gong, Y. X. Hu, J. Q. Liu and D. X. Zhou, *Sens. Actuators, B*, 2009, **140**, 190–195.
10 J. Kim and K. J. Yong, *J. Phys. Chem. C*, 2011, **115**, 7218–7224.
11 V. D. Kapse, S. A. Ghosh, G. N. Chaudhari and F. C. Raghuwanshi, *Talanta*, 2008, **76**, 610–616.
12 I. M. Szilágyi, S. Saukko, J. Mizsei, A. L. Tóth, J. Madarász and G. Pokol, *Solid State Sciences*, 2010, **12**, 1857–1860.
13 X. Xue, L. Xing, Y. Chen, S. Shi, Y. Wang and T. Wang, *J. Phys. Chem. C*, 2008, **112**, 12157–12160.
14 A. Khanna, R. Kumar and S. S. Bhatti, *Appl. Phys. Lett.*, 2003, **82**, 4388–4390.
15 I. Giebelhaus, E. Varechkina, T. Fischer, M. Rumyantseva, V. Ivanov, A. Gaskov, J. R. Morante, J. Arbiol, W. Tyrra and S. Mathur, *J. Mater. Chem. A*, 2013, **1**, 11261–11268.
16 F. Zhang, A. Zhu, Y. Luo, Y. Tian, J. Yang and Y. Qin, *J. Phys. Chem. C*, 2010, **114**, 19214–19219.
17 S. C. Lee, S. Y. Kim, B. W. Hwang, S. Y. Jung, D. Ragupathy, I. S. Son, D. D. Lee and J. C. Kim, *Sensors*, 2013, **13**, 3889–3901.
18 S. Matsuda, T. Kamo, J. Imahashi and F. Nakajima, *Ind. End. Chem. Res.*, 1982, **21**, 18–22.
19 H.-L. Yu, L. Li, X.-M. Gao, Y. Zhang, F. Meng, T.-S. Wang, G. Xiao, Y.-J. Chen and C.-L. Zhu, *Sens. Actuators, B*, 2012, **171–172**, 679–685.
20 S. D. Sartale and C. D. Lokhande, *Mater. Chem. Phys.*, 2001, **71**, 94–97.
21 C. Wu, J. Shien, J. Ma, S. Wang, Z. Zhang and X. Yang, *Semicond. Sci. Technol.*, 2009, **24**, 125012.
22 R. Swapna and S. M. C. Kumar, *Ceram. Int.*, 2012, **38**, 3875–3883.
23 J. D. Merchant and M. Covivera, *Chem. Mater.*, 1995, **7**, 1742–1749.
24 R. Swapna and S. M. C. Kumar, *J. Phys. Chem. Solids*, 2013, **74**, 418–425.
25 X. Xie, H. Yin, B. Dou and J. Huo, *Appl. Catal.*, 1991, **77**, 187–198.
26 L. Cao, S. Yang, W. Gao, Z. Liu, Y. Gong, L. Ma, G. Shi, S. Lei, Y. Zhang, S. Zhang, R. Vajtai and P. M. Ajayan, *Small*, 2013, **9**, 2906–2910.
27 P. Afansoev, G.-F. Xia, G. Berhault, B. Jouguet and M. Lacroix, *Chem. Mater.*, 1999, **11**, 3216–3219.
28 I. Shakir, M. Shahid and D. J. Kang, *Chem. Commun.*, 2010, **46**, 4324–4326.
29 S. Y. Bae, H. C. Choi, C. W. Na and J. Park, *Appl. Phys. Lett.*, 2005, **86**, 033102.
30 C. S. Rout, S. H. Krishna, S. R. C. Vivekchand, A. Govindaraj and C. N. R. Rao, *Chem. Phys. Lett.*, 2006, **418**, 586–590.
31 C. S. Rout, A. R. Raju, A. Govindaraj and C. N. R. Rao, *J. Nanosci. Nanotechnol.*, 2007, **7**, 1923–1929.
32 C. S. Rout, G. U. Kulkarni and C. N. R. Rao, *J. Nanosci. Nanotechnol.*, 2009, **9**, 5652–5658.
33 X. Wang, W. Liu, J. Liu, F. Wang, J. Kong, S. Qiu, C. He and L. Luan, *ACS Appl. Mater. Interfaces*, 2012, **4**, 817–825.
34 N. Barsan and U. Weimar, *J. Electroceram.*, 2001, **7**, 143–167.
35 O. Lupan, L. Chow, Th. Pauporté, L. K. Ono, B. R. Cuenya and G. Chai, *Sens. Actuators, B*, 2012, **173**, 772–780.
36 N. Yamazoe, J. Fuchigami, M. Kishikawa and T. Seiyama, *Surf. Sci.*, 1979, **86**, 355–344.
37 S.-C. Chang, *J. Vac. Sci. Technol.*, 1980, **17**, 366–369.
38 Z. Sun, H. Yuan, Z. Liu, B. Han and X. Zhang, *Adv. Mater.*, 2005, **17**, 2993–2997.
39 J. Deng, J. Ma, L. Mei, Y. Tang, Y. Chen, T. Lv, Z. Xu and T. Wang, *J. Mater. Chem. A*, **1**, 12400–12403.
40 G. Cui, M. Zhang and G. Zou, *Sci. Rep.*, 2012, **3**, 1–8.
41 L. Zhou, F. Shen, X. Tian, D. Wang, T. Zhang and W. Chen, *Nanoscale*, 2013, **5**, 1564–1569.
42 M. Munz, M. T. Langridge, K. K. Devarepally, D. C. Cox, P. Patel, N. A. Martin, G. Vargha, V. Stolojan, S. White and R. Curry, J. *ACS Appl. Mater. Interfaces*, 2013, **5**, 1197–1205.
43 J. Kim, W. Kim and K. Yong, *J. Phys. Chem. C*, 2012**, 116**, 15682–15691.
44 L. A. Patil and D. R. Patil, *Sens. Actuators, B*, 2006, **120**, 316–323.
45 D. J. Late, Y.-K. Huang, B. Liu, J. Acharya, S. N. Chirodkar, J. Luo, A. Yan, D. Charles, U. V. Waghmare, V. Dravid and C. N. R. Rao, *ACS Nano*, 2013, **7**, 4879–4891.
46 P. Sun, Y. Liu, X. Li, Y. Sun, X. Liang, F. Liu and G. Lu, *RSC Adv.*, 2012, **26**, 9824–9829.
47 X. Liu, J. Zhang, X. Guo, S. Wu and S. Wang, *Nanoscale*, 2010, **2**, 1178–1184.
48 S.-J. Kim, I.-S. Hwang, C.-W. Na, I.-D. Kim, Y.-C. Kang and J.-H. Lee, *J. Mater. Chem.*, 2011, **21**, 18560–18567.
49 H.-J. Kim, K.-I. Choi, A. Pan, I.-D. Kim, H.-R. Kim, K.-M. Kim, C.-W. Na, G. Cao and J.-H. Lee, *J. Mater. Chem.*, 2011, **21**, 6549–6555.
50 H. G. Moon, Y.-S. Shin, D. H. Kim, H. Y. Jeong, M. Jeong, J. Y. Jung, S. M. Han, J. K. Kim, J.-S. Kim, H.-H. Park, J.-H. Lee, H. L. Tuller, S.-J. Yoon and H. W. Jang, *Sci. Rep.*, 2012, **2**, 588.
51 T. Jinkawa, G. Sakai, J. Tamaki, N. Miura and N. Yamazoe, *J. Mol. Catal. A*, 2000, **155**, 193–200.

Journal of Materials Chemistry A Accepted Manuscript

 This journal is © The Royal Society of Chemistry 2012

ToC

Selective, sensitive, and reversible H_2S sensors

using Mo-doped ZnO nanowire networks

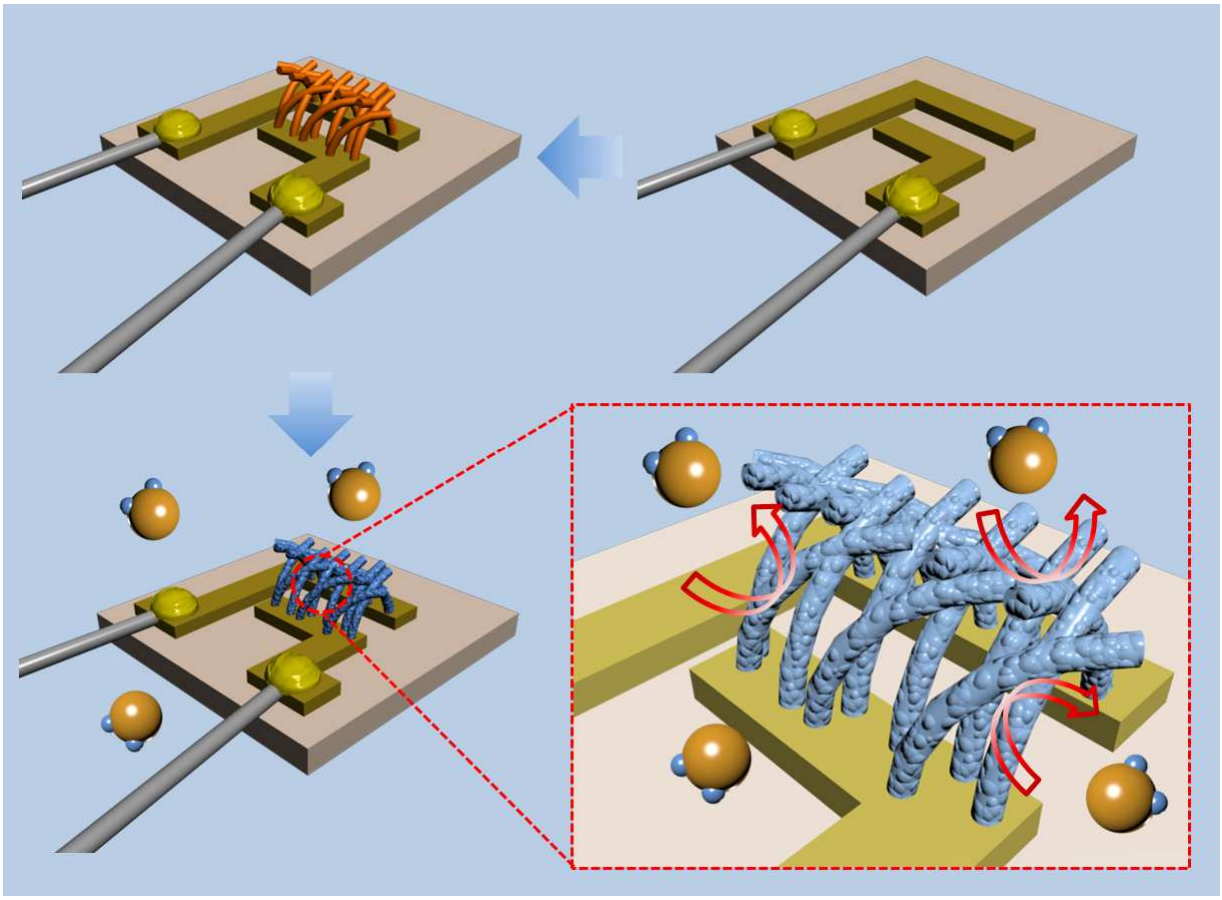

Selective, sensitive and reversible detection of H_2S was achieved using Mo-doped ZnO nanowire networks prepared by CVD and SILAR method.

Journal of Materials Chemistry A Accepted Manuscript